Neutron Monitor Response Functions

J.M. Clem
Bartol Research Institute, University of Delaware, Newark, DE, USA

L.I. Dorman
IZMIRAN, Moscow, Russia; Technion, Haifa, and Israel Cosmic Ray Center, affiliated with Tel Aviv University

Abstract.

The neutron monitor provides continuous ground-based recording of the hadronic component in atmospheric secondary radiation which is related to primary cosmic rays. Simpson (1948) discovered that the latitude variation of the secondary hadronic component was considerably larger than the muon component suggesting the response of a neutron monitor is more sensitive to lower energies in the primary spectrum. The different methods of determining the neutron monitor response function of primary cosmic rays are reviewed and discussed including early and recent results. The authors also provide results from a new calculation (Clem, 1999) including angle dependent yield functions for different neutron monitor types which are calculated using a simulation of cosmic ray air showers combined with a detection efficiency simulation for different secondary particle species. Results are shown for IGY and NM64 configurations using the standard $^{10}BF_3$ detectors and the new ^3He detectors to be used in the Spaceship Earth Project (Bieber et al., 1995). The method of calculation is described in detail and the results are compared with measurements and previous calculations. A summary of future goals is discussed.

Keywords: Neutron Monitor, Response Function, Cosmic Rays

1. Introduction

In order to understand the ground-based neutron monitor as a primary particle detector a relationship between the count rate and primary flux must be established. Primary particles, not rejected by the geomagnetic field, enter the atmosphere and undergo multiple interactions resulting in showers of secondary particles which may reach ground level and be detected by a neutron monitor. Therefore a yield function must incorporate the propagation of particles through the Earth's atmosphere and the detection response of a neutron monitor to secondary particles such as neutrons, protons, muons and pions. The response functions can then be determined by convolving the cosmic ray spectra with the yield function. The expected count rate from latitude surveys can be calculated by integrating the resulting response functions.

After the invention of the neutron monitor by Simpson (1948), the concept of response functions was introduced by Fonger (1953), Brown

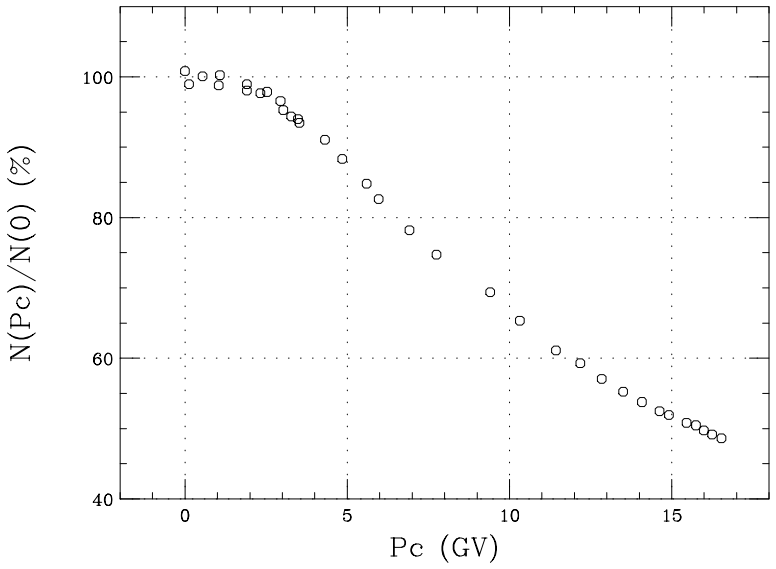

Figure 1. Count rate recorded on the Italian Antarctic Program 3-NM-64 survey during 1996-97 (Villoresi, 1997).

(1957) and Dorman (1957) , and since then, a number of ventures have been taken to fully characterize these functions and to understand their inherent features. Complete interpretation requires knowledge of the detection efficiency, atmospheric particle transport, primary composition and energy spectrum, and geomagnetic particle transport. This paper focuses specifically on particle transport through the atmosphere and the detection efficiency of a neutron monitor.

The integral response function (count rates) is directly measured during a neutron monitor latitude survey, which is a mobile station that records counting rates while traversing a range of geomagnetic cutoffs (Moraal et al., 1989, and references therein). An example of count rates recorded during a typical survey is displayed in Figure 1, revealing a strong correlation with geomagnetic cutoff. Equation (1) provides a simplified mathematical description of the relationship between parameters relevant to a latitude survey in the usual approximation:

$$N(P_C, z, t) = \int_{P_C}^{\infty} \sum_i (S_i(P, z) j_i(P, t)) dP = \int_{P_C}^{\infty} W_T(P, z, t) dP \qquad (1).$$

where $N(P_C, z, t)$ is the neutron monitor counting rate, P_C is the geomagnetic cutoff, z is the atmospheric depth and t represents time.

$S_i(P,z)$ represents the neutron monitor yield function for primaries of particle type i and $j_i(P,t)$ represents the primary particle rigidity spectrum of type i at time t. It should be emphasized that the geomagnetic cutoff P_C and the yield function $S_i(P,z)$ both depend on the arrival direction of the incident primary particles. The vertical cutoff rigidity usually suffices as an adequate approximation to the lower-limit rigidity of the primary spectrum, however there are some documented cases where the contribution of obliquely incident primaries are responsible for anomalies observed in latitude surveys (Clem et al., 1997 and Stoker et al., 1997). The total response function $W_T(P,z,t)$ on the right hand side of Equation (1) is defined as the summed product of $S_i(P,z)$ and $j_i(P,t)$, and has a maximum value in the range of 4-7 GV at sea-level depending on the solar modulation epoch at time t. It should be explicitly noted that a latitude survey can only provide a response function at the time of the survey since the primary spectrum $j_i(P,t)$ is time correlated with the 22 year solar cycle (Fisk et al., 1969 and Garcia-Munoz et al., 1986) and is also subject to sudden transient effects such as Forbush decreases or solar energetic particles. The study of response functions has lead to improved understanding of the quantities mentioned above and of the neutron monitor operation. including the additional information gained from multiplicity counts. A brief review of the neutron monitor design is discussed.

2. Background and Review of the Neutron Monitor Design

In a neutron monitor, neutron sensitive proportional tubes, surrounded by moderator material and a lead target, detect near-thermal neutrons produced locally from interacting incident particles. Even though neutrons do not leave an ion trail in the proportional tube, the absorption of a neutron by a nucleus is usually followed by the emission of charged particles which can be detected. A proportional tube filled with either $^{10}BF_3$ or ^{3}He gas responds to neutrons by the exothermic reaction ^{10}B(n,α)^{7}Li or ^{3}He(n,p)^{3}H. The reaction cross-sections for both nuclei is inversely proportional to the neutron speed, having a thermal endpoint (0.025eV) of roughly 3840 barns and 5330 barns respectively, as shown in Figure 2.

Surrounding each counter is a moderator which serves to reduce the energy of neutrons, thus increasing the probability of an absorption inside the counter while also providing a reflecting medium for low energy neutrons. The moderator material is chosen to contain a significant fraction of hydrogen as the energy loss per neutron elastic collision increases with decreasing atomic mass ($\frac{dE}{E} = \frac{4A\cos^2\Theta_{recoil}}{(1+A)^2}$). The neutron elastic

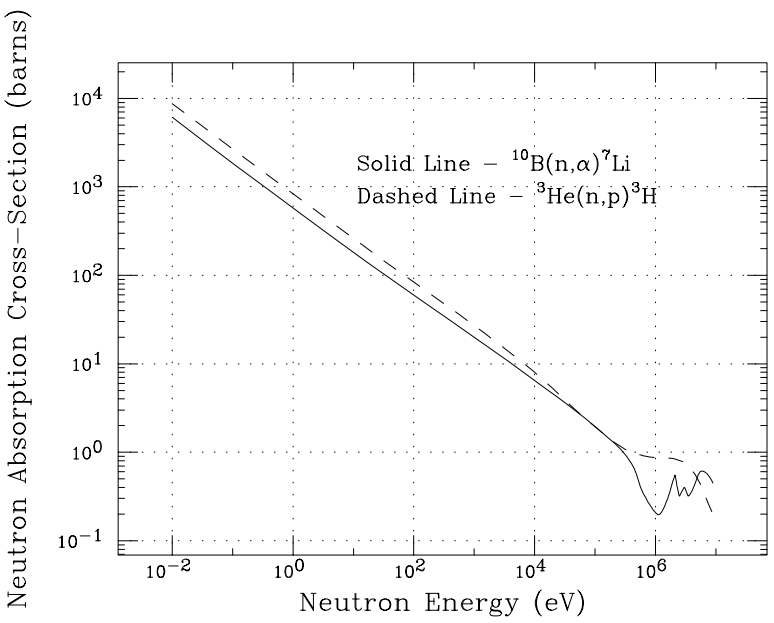

Figure 2. The reaction cross section versus neutron energy for ^{3}He and ^{10}B.

interaction pathlength of hydrogen in typical moderator materials is roughly 1 cm ($E_n \leq 1$ MeV) and each interaction reduces the incident neutron energy by a factor of 2 on the average. The lead producer, which surrounds the moderator, provides a thick large-nucleus target for inelastic interactions in which secondary neutrons are produced. A high atomic mass (A) is preferred in the producer as the neutron production rate per unit mass of a material is roughly proportional to A^{γ} with $\gamma \sim 0.7$ in the 100-700 MeV incident energy range and slowly decreasing with increasing energy ($E \geq 400$ GeV, $\gamma \sim 0.0$). (Shen, 1968). Surrounding the lead is an outer moderator, usually referred to as to the reflector, which serves to contain low energy neutrons produced in interactions within the lead as well as reject unwanted low energy neutrons produced in the local surroundings from entering into the detector.

In some stations each counter has a dedicated electronics interface allowing the ability to measure multiplicity coincidences between counters which is the simultaneous occurrence of counts in multiple counters. The count rates of different multiplicity levels can then be recorded and analyzed (Raubenheimer et al., 1980). The neutron monitor's peak energy response to secondary particles increases with increasing mul-

tiplicity, suggesting each multiplicity level is related to the primary spectrum through a different yield function.

Generally the most unstable component of the neutron monitor is the Earth's atmosphere which must be closely monitored at each station. The response of a neutron monitor is dependent on the air mass over-burden, and therefore meteorological changes can affect the counting rate. Even though the neutron monitor design is optimized to detect secondary neutrons from interactions occurring primarily in the producer, atmospheric corrections are still necessary at the few percent level as discussed in the next section. For further details on neutron monitor design see Stoker et al. (2000)

3. Atmospheric Effects

Atmospheric corrections for neutron monitors are based on theory and experimental investigations of meteorological phenomena that affect the passage of particles through the atmosphere (Dorman, 1970, Hatton, 1971 and Iucci et al., 1999). The meteorological effects that are associated with changes in the air mass overburden are obviously the most important. During stable atmospheric conditions, the barometric pressure recorded at the monitor site is a good measure of the air overburden and an approximate correction can be written as

$$dN = -\alpha N\, dp \tag{2}$$

where α is the attenuation or barometric coefficient, dN is change in the count rate N and dp is the change of the barometric pressure. In general the barometric coefficients used at each neutron monitor station are determined empirically, however these values can be calculated through Monte Carlo simulations. Direct measurements have shown that the barometric coefficient is a function of latitude and altitude (Moraal et al., 1989 and Raubenheimer et al., 1974) which increases with altitude below 600mm-Hg and decreases with altitude above 600mm-Hg (Carmichael et al., 1969b). Observations have also shown that the barometric coefficient varies with the solar cycle (Hatton, 1971 and references therein).

The barometric coefficient is actually a weighted sum of individual barometric coefficients for each secondary component that contributes to the counting rate. These individual coefficients are directly coupled to the fundamental properties that define particle transport through the atmosphere such as hadronic interactions, energy loss, scattering and particle decay length. Since the resulting effect from each of these mechanisms is energy dependent, the barometric coefficient is expected

to vary to some degree with the rigidity cutoff and the shape of the primary spectrum (modulation level). The energy, angular and species distribution of secondary particles in the atmosphere varies greatly with depth therefore the barometric coefficient is also expected to vary in altitude. As an example, equation (2a) provides the barometric coefficient values derived empirically from a fit to coefficients reported by 11 sea-level neutron monitor stations with various cutoffs during 1995 (Clem et al., 1997).

$$\alpha = 0.983515 - 0.00698286 P_c \qquad (2a)$$

where α is in units of percent per mm Hg and P_c is units of GV(gigavolts).

A change in the density-altitude profile, usually caused by temperature changes at different altitudes, will vary the population of unstable species produced in the atmosphere. The most significant effect is the change in the ratio of the number of pion interactions to pion decays. This effect alters the distribution of species types which contribute to the count rate and therefore, varies the effective barometric coefficient. Unlike the pressure effect, the temperature effect is related to a series of coefficients defining the mass distribution between the first interaction point and ground level (Dorman, 1957, Bercovitch et al., 1966). At sea-level the effect is much less than in the muon counter array (Duldig, 2000) mainly due to the relatively low contribution of muons and pions to the neutron monitor count rate.

It also has been reported that measurements of atmospheric pressure are significantly affected by strong turbulent winds due to the Bernoulli effect. Consequently, the standard pressure corrections (equation 2) for neutron monitor data for the effects of air overburden changes can lead to erroneous results during high wind conditions. Various techniques for wind speed corrections have been proposed which improve the reliability of pressure corrected data (Bütikofer et al., 1999, Iucci et al., 1999 and references therein).

Particular care in monitoring meteorological phenomena must be taken during latitude surveys. Neglecting the accuracy in these observations can produce serious systematic effects in the resulting response function that are derived from the pressure corrected count rates.

4. Review on Determining Response Functions

The methods for determining a neutron monitor response function can be separated into 3 different categories; 1) parameterization of latitude survey observations, 2) theoretical calculation and 3) Monte Carlo simulation of cosmic ray transport through the atmosphere and

the neutron monitor detector using fundamental knowledge of high energy physics, nuclear physics and geophysics. The limitations and advantages of each method are discussed below.

4.1. Parameterization Method

The parameterization method directly determines an approximation to the total response function by fitting a chosen function to the count rates measured during a neutron monitor latitude survey (Raubenheimer et al., 1981). Lockwood et al. (1974) derived the response function through a piece-wise function to match the slope changes in latitude survey observations while others have used simple polynomials in log-log space to fit to latitude surveys. However, the most commonly used fitting function is the Dorman function (Dorman, 1970) shown as equation (3). Numerically, the Dorman Function represents most latitude surveys fairly accurately (Stoker, 1995, Moraal et al., 1989), particularly when the geomagnetic cutoff values are corrected for obliquely incident particles (Clem et al., 1997, Stoker et al., 1997). Futhermore, the upper and lower limits in the Dorman function are physically acceptable. However, the simplicity of this technique, which uses only 3 free parameters, is a double edged sword. It is very stable and simple to apply, but the fact that very little physics was used to construct the Dorman function may cause unphysical smoothing of data. Moreover, this analysis limits the amount of information that can be isolated and extracted such as the primary spectrum, atmospheric transport and detection efficiency.

In their extensive analysis of latitude surveys, Nagashima et al. (1989) constructed a modular fitting function by combining the modulation function, galactic spectrum, atmospheric transport and detection efficiency through separate parameterizations based on the theories and observations of the process. This method allows isolation of each term (ignoring correlation effects) and the ability to verify physical representation through comparing the derived quantities with other observations and calculations. The resulting response functions are shown in figure 3. The analysis was quite successful in reproducing latitude survey observations, however the derived galactic spectrum is somewhat flatter than that obtained from balloon and space measurements.

In general, the parameterization method restricts direct determination of response functions to depths of latitude survey observations which are usually performed at sea-level and 30,000 ft (Nagashima et al., 1989). There are only 3 documented airborne surveys that have been performed at mountain altitudes (5000-10,000 ft) (Sandström, 1958 and Carmichael et al., 1969a), while a good fraction of monitor

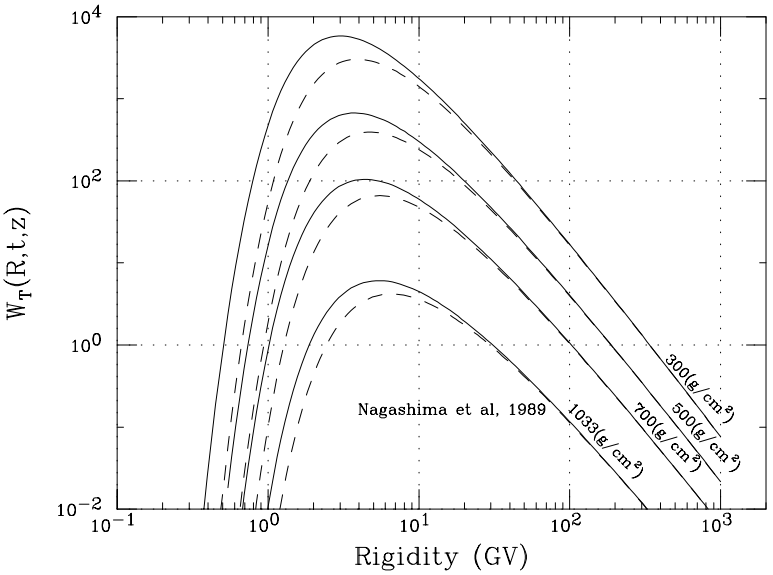

Figure 3. Total differential response function of a neutron monitor for different atmospheric depths during solar minimum (solid lines) and maximum (dashed lines) as derived by Nagashima et al. (1989) .

stations reside on mountains. Moreover, the choice of functional form to be used in a parameterization analysis can bias the final fit, however with special care as with Nagashima et al. (1989) biasing effects can be easily recognized and corrected.

4.2. Theoretical Calculation Method

The calculation method does not necessarily rely on observational data, but instead attempts to quantify all the fundamental physical mechanisms that significantly affect the transport of radiation through the atmosphere. This method is obviously more complex to perform and requires very accurate input data such as interaction cross-sections, interaction kinematics, secondary multiplicities, secondary angular distributions, energy loss effects, multiple Coulomb scattering and the atmospheric density profile just to name a few. Most of the required input data have been measured to the accuracy needed to perform this calculation, however a single inaccurate input can lead to systematic errors. The major advantage to this method is that the range of input parameter values is limited to the accuracy of the measured input data and each parameter has a fundamental physical definition. In most

cases however, the physical fluctuations and correlations in the transport equations are not implemented properly and instead approximate independent Gaussian errors are propagated through the calculation leading to systematic effects in determining mean values. Dorman and Yanke (1981) developed an atmospheric cascade calculation to determine yield functions for neutron monitor stations located at mountain altitudes. Ignoring scattering effects, and pion and muon production, they constructed transport equations of differential particle multiplicity and determined a solution by the method of successive generations. The solution was then used to determine the yield function and response functions. In comparison with other work, this result is more consistent with sea-level observations than higher elevations, possibly from neglecting the effects mentioned above.

Yanke (1980), Belov (1997) and Belov (1999) parameterized the results of Dorman and Yanke (1981) using a depth dependent Dorman function as shown in equation (3)

$$N(R) = N(0)(1 - \exp(-\alpha P_C^{-\kappa+1})) \tag{3}$$

where P_C is the cut-off rigidity and α and κ are depth dependent parameters. The first derivative of equation (3) gives the total response function

$$W(P_C) = \frac{-dN}{N(0)dP_C} = \alpha(\kappa - 1)\exp(-\alpha P_C^{-\kappa+1})P_C^{-\kappa}$$

having a maximum value

$$W_{max} = \kappa P_{max}^{-1}\exp\Big(-\frac{\kappa}{\kappa-1}\Big), \text{where } P_{max} = \Big(\frac{\alpha(\kappa-1)}{\kappa}\Big)^{1/(\kappa-1)}$$

The median rigidity is

$$P_{med} = (\alpha/\ln 2)^{1/(\kappa-1)}$$

For solar minimum the derived parameters are expressed by the following expression

$$\ln\alpha = 1.84{+}0.094h{-}0.09\exp(-11h), \kappa = 2.40{-}0.56h{+}0.24\exp(-8.8h)$$

and for solar maximum activity

$$\ln\alpha = 1.93{+}0.15h{-}0.18\exp(-10h), \kappa = 2.32{-}0.49h{+}0.18\exp(-9.5h)$$

where h is atmospheric depth in bars. These functions provide a good representation of the Dorman and Yanke (1981) calculation in the

rigidity range of $2 < R < 50GV$. The least square fit of this parameterization was applied to calculated data only within this range therefore results calculated outside of these limits are unphysical.

The detection efficiency of neutron monitors can be separately determined using similar techniques. Hatton (1971) calculated the particle transport through a neutron monitor structure and determined the neutron monitor response to ground-level particles. This required the combining of results from three different calculations: 1) the probability of a particle punching through the reflector and interacting within the lead, 2) the mean number of neutrons produced per interaction and 3) the probability for detecting a neutron. The results provided the average number of counts per incident proton and neutron for NM-64 and IGY configurations as discussed in section 5.1. The muon contribution was determined as a percentage to the total counting rate. This result has become the standard detection response adopted by numerous workers.

4.3. Monte Carlo Method

A Monte Carlo simulation of particle transport can be constructed if the probability distribution is known for each process. In this method, particle transport is simulated as a sequence of flights along a trajectory where each flight length is a random variable depending on the process cross-section of the material. As with a theoretical calculation, the Monte Carlo method does not necessarily rely on observational data and requires very accurate input data of fundamental transport quantities. The major difference is that the Monte Carlo attempts to simulate all the significant physical mechanisms in the expected time sequence producing a history of particle tracks. In general the Monte Carlo is used to generate a population of cascades and the history of each cascade in the form of particle tracks is recorded. The recorded data can then be used to determine spectra fluences scored for different particle species and then the results are weighted by the detection efficiency of a neutron monitor to determine the counting rate.

One of the first successful attempts in developing a Monte Carlo to simulate cosmic ray cascades was the work of Debrunner and coworkers (Debrunner et al., 1968, Flückiger, 1977, Raubenheimer et al., 1977). The results from this work are fairly consistent with the observed secondary proton spectrum and latitude surveys. This Monte Carlo also has been used to determine the detection efficiency of modified NM-64 neutron monitors and to study the multiplicity observations in latitude surveys (Raubenheimer et al., 1980). They reported that good

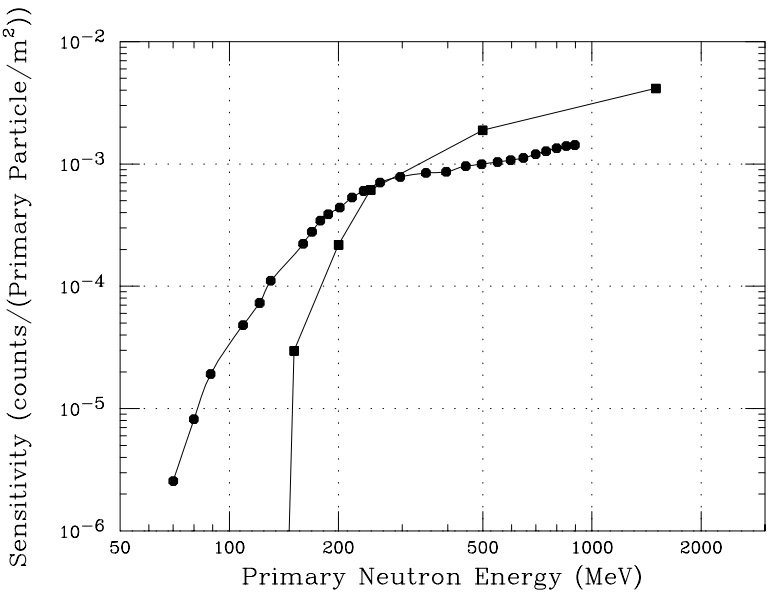

Figure 4. Comparison of solar neutron yield functions at the Climax Neutron Monitor station as function of incident energy at the top of the atmosphere with slant depth of 776g/cm^2. Shibata (1994) results are represented by the circle symbols and Debrunner et al. (1997) results are shown as squares.

qualitative agreement is found between observational and simulated results.

The input data in this Monte Carlo has since been updated and the code has been modified to transport solar neutrons (Debrunner et al., 1997). Shibata (1994) developed an extensive Monte Carlo calculation independent of the above work to also simulate the transport of primary neutrons. Figure 4 displays yield functions determined from both Monte Carlo calculations for conditions expected at the Climax neutron monitor station with primary neutrons arriving at 28.8^o with respect to the zenith at the station. As shown there are significant differences in the low and high energy regions. This could be the result of implementing different treatments of elastic neutron-nucleus collisions and obliquely incident primaries. The attenuation of neutrons through thick carbon slabs has been measured using an accelerator at the Research Center for Nuclear Physics, Osaka University. This work should help resolve differences between the two simulations (Koi et al., 1999).The details of solar primary neutrons are beyond the scope of this chapter and will

not be further discussed, however Debrunner (2000) and the above are excellent references to the subject.

Over the years, numerous particle accelerator sites have supported groups to construct software tools to simulate elementary particle transport using the available data. After much work and cross-checking some of these software packages have become very accurate, but are usually specialized for applications associated with the facilities. There are a few packages, however that are applicable outside this domain. One such package entitled FLUKA (FLUcuating KAscades) (Fassò et al., 1993,1997) is applicable to the 3-dimensional transport of particles through the atmosphere and a neutron monitor with energies ranging 0.02eV to 20TeV (Clem et al., 1997, Clem, 1999). As an example, the FLUKA package was used to determine the detection response of different neutron monitors and the transport of particles through atmosphere. These results will be discussed and compared to work mentioned in the following section.

5. Monte Carlo simulation based on FLUKA

5.1. Detection Response

The neutron monitor (NM) detection response for secondary particles at ground level was determined using FLUKA combined with programs written by Clem (1999) to simulate the proportional tube and electronics response to energy deposition in the gas. The standard dimensions and composition of materials of an IGY and NM-64 were used as input to the geometry (Hatton, 1971). Initially, a four meter diameter parallel beam of mono-energetic particles at a fixed angle fully illuminates the neutron monitor and is repeated for different incident beam angles, initial energy and particle species including neutrons, protons, positive and negative pions and muons. Data are stored for every beam particle that produces a minimum value of energy deposited in any counter. These data are then used to generate a pulse height distribution which is integrated (with dead-time and pile-up effects) to determine the total number of counts per beam luminosity (number of beam particles/beam area).

Figure 5 displays the resulting detection efficiency of a NM-64 with $^{10}BF_3$ counters for 6 different particle species in the vertical incident direction. As shown the detector response is optimized to measure the hadronic component of ground level secondaries. The NM response from muons above 1 GeV is roughly 3.5 orders of magnitude below the hadrons. In this energy region, the primary mechanisms for muon

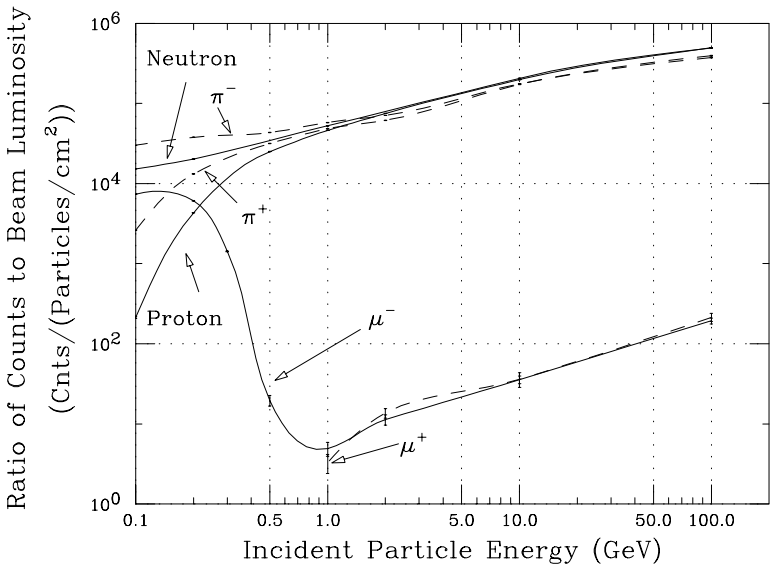

Figure 5. Standard (BP-28 proportional tubes) NM64 calculated detection efficiency for secondary particles arriving in the vertical direction.

induced counts are neutron production in photo-nuclear interactions and electromagnetic showers resulting in multiple ionization tracks in a counter. Below 1 GeV, stopping negative charge muons are captured by a lead nucleus into a mesic orbit and absorbed by the nucleus. The de-excitation of the nucleus occurs with the emission of neutrons which is reflected in the rise in detection efficiency with decreasing energy.

As expected, there is practically no difference in the response between neutrons and protons in the high energy region, while at lower energies the ionization energy loss of protons becomes significant, greatly reducing the probability of an interaction, which is reflected in the decreasing detection efficiency. Positive and negative charged pions produce almost identical responses at high energies while at lower energies negative pions undergo nuclear capture like negative muons. However, the pion absorption time after capture is much less, compensating for the pions shorter decay-time as reflected in the rise in negative pion efficiency. It also should be noted that the pion inelastic cross sections are smaller than those of a nucleon in the high energy region and, therefore, have a lower detection response since the NM vertical lead depth is only 80% of the nucleonic inelastic interaction pathlength.

Shown in Figure 6 is the resulting detection efficiency for protons and neutrons in NM-64 and IGY neutron monitors compared with

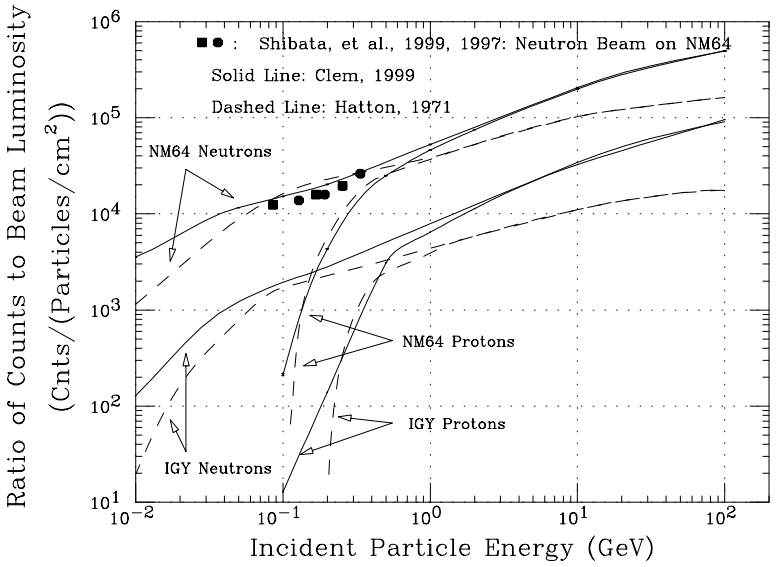

Figure 6. Comparison of Neutron Monitor detection efficiency data and calculations.

Hatton's calculation (1971) and NM-64 accelerator data (Shibata et al., 1997, 1999). The dashed lines represent Hatton's calculation and solid lines represent the present calculation. Unfortunately, the data lie in the only region where the calculations agree and the data are consistent with both calculations. Coincidently, in this region lies the peak response for both NM-64 and IGY monitors when ground-level spectra are considered. It is not clear why the two calculations differ outside this region.

Figure 7 displays the calculated detection response of an NM-64 for vertical incident neutron and proton beams. This plot shows simulations for the traditional BP-28 detector employing $^{10}BF_3$ and for a detector using ^{3}He designed to have a similar response (Clem, 1999, Pyle et al., 1999). The calculated ^{3}He NM-64 response is systematically slightly higher. Pyle et al. (1999), reporting preliminary results from a recent latitude survey, suggest that the ^{3}He NM-64 response is roughly 5% higher than predicted by this calculation. Various small effects in the survey system not included in this simulation could contribute to this difference (see Stoker et al., 2000 for detector specifications).

Figure 8 shows the detection response of an IGY, BP-28 NM-64 and ^{3}He NM-64 for incident neutrons extended down to near thermal energies. Both NM-64 types agree quite well for the full energy range with curves almost superimposed, however the IGY has a different

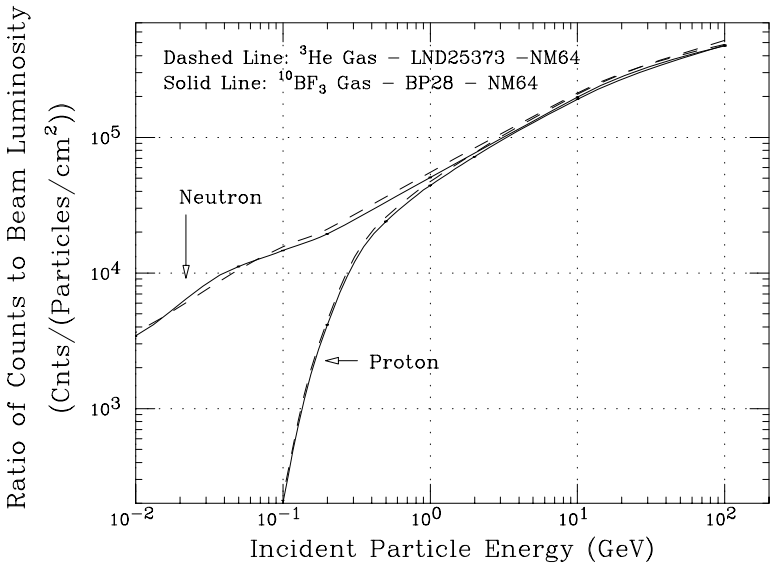

Figure 7. Calculated detection efficiency of ^{3}He NM-64 and $^{10}BF_3$ NM-64 for protons and neutrons.

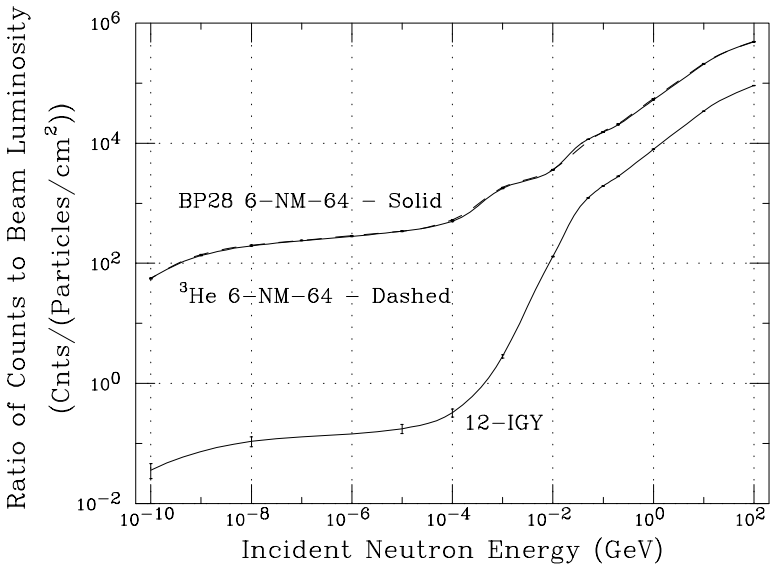

Figure 8. A comparison of calculated detection efficiency of incident neutrons over full range of energies.

response in both magnitude and shape. The shapes of the curves are very similar for energies above 100 MeV, however, below this energy the shape differences are significant mainly due to the thicker reflector used in the IGY. As shown, the additional thickness is much more efficient at preventing low energy neutrons from entering the detector region, however this increases the number of carbon inelastic collisions reducing the average neutron yield per interaction.

5.2. Particle Transport through the Atmosphere

The propagation of primary particles through the Earth's atmosphere was also simulated with FLUKA. Primary particles are filtered through either a uniform or angle dependent effective cutoff rigidity (Clem et al., 1997, Cook et al., 1991, Lin et al., 1995, Smart et al., 2000) calculated for each geographical location, and the surviving particles are transported through the atmosphere. The simulated ground-level particle intensities, folded with the calculated neutron monitor detector response are then used to calculate a geographically dependent counting rate. The details of the simulation are described below.

Mono-energic primary protons and alphas are generated at different fixed incident directions within the rigidity range of 1 GV — 2000 GV. Alpha particles are initially transported with a separate package called HEAVY (Engel el al., 1992) to simulate fragmentation. This package interfaces with FLUKA to provide interaction starting points for each nucleon originating from a helium nucleus.

The atmosphere is divided into sixty (bottom boundary radius = 6378.14 km) concentric spherical shells with differing radii and density to simulate the actual density profile (Gaisser, 1990) with a vertical total 1033g/cm^2 column density for sea level and 305 g/cm^2 for 9.1 km (30,000 ft). Above 500 meters the atmospheric composition (Zombeck, 1982) is constant with a 23.3% O_2, 75.4% N_2 and 1.3% Argon distribution by mass while below 500 meters a varying addition of H_2 from 0.06% at sea-level to 0.01% at 500 meters is included to account for the abundance of water vapor.

The outer air-space boundary is radially separated by 65 kilometers from the inner ground-air boundary. A single 1 cm^2 element on the air-space boundary is illuminated with primaries. This area element defines a solid angle element with respect to the center of the Earth which subtends a slightly smaller area element on the ground. Particle intensity at sea-level or 30,000 ft-level is determined by superimposing all elements on the bottom boundary. Due to rotational invariance this process is equivalent to illuminating the entire sky and recording the

flux in a single element at ground level, but requires far less computer time.

An event data base was accumulated from outputs of many runs with different rigidities, incident angles and primary types. The information for all generated primaries and resulting particles at sea-level was stored in a format such that the sea-level particles could be linked to the parent primary. This format allows the same data base to be used for calculations with different rigidity cutoffs.

The propagation calculation ignores some effects that should be pointed out:

- The geomagnetic field is ignored during transport through the atmosphere. For instance, the trajectory of a vertical incident 5GV primary proton near the geomagnetic equator is deflected by roughly 8 degrees over an arc length of 50km
- The additional overburden grammage from typical housing structures for neutron monitor such as walls and ceiling is disregarded.
- The Earth's surface is treated as a perfect particle absorber (black hole material) and splash albedo is ignored from ground interactions.

Admittedly, some of these effects are small, but the combination could produce a significant difference in the results. Future projects will involve work implementing these mechanisms into the full calculation.

As a check, sea-level vertical particle fluxes (Rossi, 1948) are calculated from the event database and compared to published data (Allkofer and Grieder, 1984). The absolute normalization of the simulated flux is determined from the number of generated primaries, weighted according to a standard primary spectrum (Seo et al., 1991, Badhwar et al., 1996), with no free parameters in the comparison. The particle types compared are muons, protons and neutrons. Clem et al. (1997) show that the observed and simulated data agree fairly well which provides confidence in the accuracy of the atmospheric particle transport for this simulation.

5.3. Yield Functions

To convert ground-level particle intensities to a neutron monitor counting rate one must know the detection efficiency of a neutron monitor system. As described in the detection response subsection, the mean number of counts per incident secondary particle for a neutron monitor detector as a function of incident angle, energy and particle type has

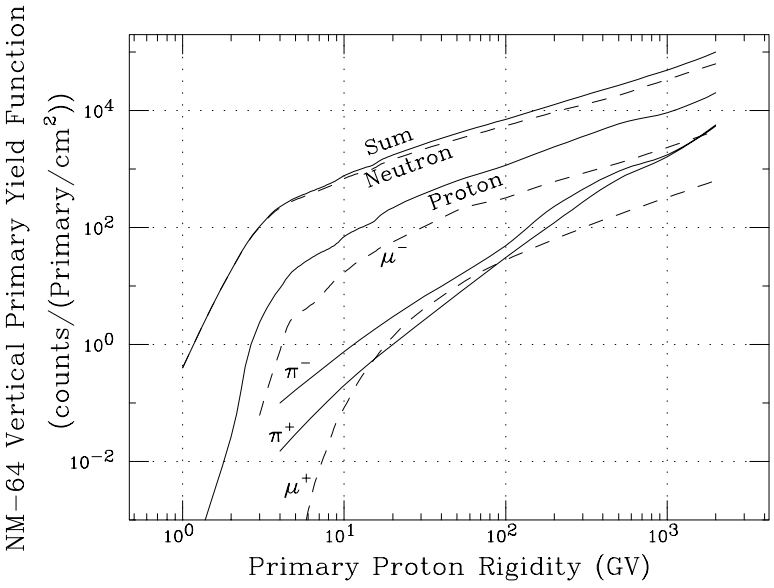

Figure 9. Calculated yield function spectra of NM-64 counts at sea level from vertical incident primary protons is shown (top line). The individual contributions made by secondary components to the vertical proton yield function are separated into different curves. The dominating contribution is from secondary neutrons.

been calculated. A yield function is then determined by calculating the average number of neutron monitor counts per incident primary which is essentially the neutron monitor detection efficiency of primary particles.

The calculated NM-64 yield function at sea-level for vertical incident primary protons is shown in Figure 9 as the top curve. The yield units are the average number of NM-64 counts for every incident primary particle per cm^2. The contributions from different secondary particle species are separated into different curves. As shown, the dominating contribution to the yield function is from secondary neutrons, however protons and negative muons contribute a significant fraction above 5GV while the pion contribution increases with energy becoming a significant component above 50GV.

Figure 10 displays the yield function calculation at sea level for 3 different conditions. The solid lines in both left and right frames represent the NM-64 yield function from primary protons arriving at different fixed incident angles with respect to the zenith at the top of the atmosphere. The top curve represents vertical incident primaries with 0^o, the middle curve represents the 45^o incident direction and the bottom curve is 60^o. The dashed lines in the left frame represent the NM-64 yield function for primary alpha particles while the dashed

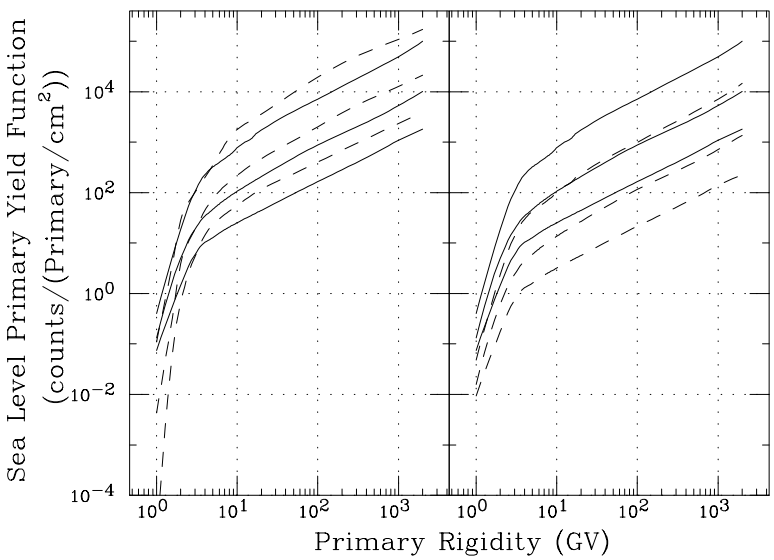

Figure 10. In the right frame, the yield function of an IGY (dashed lines) and NM64 (solid lines) from primary protons arriving at 0^o, 45^o and 60^o incidence are shown. In the left frame, the yield function of NM64 from primary alphas (dashed lines) are also shown for same arriving incidence. The solid lines shown in both frames are the same.

lines in the right frame represent the IGY yield function for primary protons. As expected, the smaller IGY results in a lower yield function, but having a similar shape. For the same high rigidity, one would expect alphas to have a higher yield due to having a larger total kinetic energy than protons, however at lower rigidities the higher ionization energy loss of alphas is more effective in preventing inelastic collisions than for protons, which is reflected in the cross-over in yields.

6. Comparison of Results

For comparison primary proton yield functions as a function of vertical cutoff derived from different methods are shown together in Figure 11 for a NM-64 at sea-level. For many purposes, use of the vertical cutoff (i.e. the cutoff for a vertically incident particle) is sufficient, but in reality the cutoff rigidity depends upon direction of incidence. Since cosmic rays arrive almost isotropically there is a large population of obliquely incident primaries. Atmospheric absorption increases rapidly with increasing slant-depth, so the first approximation is to consider only the particles incident vertically. However, as shown in the previous section, response to off-vertical particles is finite, and the primary in-

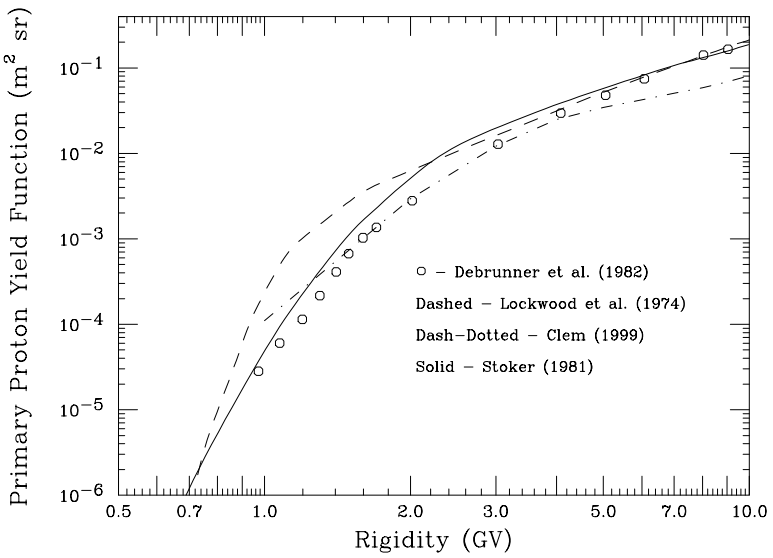

Figure 11. A comparison of different proton yield function for a NM-64 at Sea-Level. The yield functions derived by Lockwood et al. (1974) and Stoker (1981) were determined using similar parameterization methods while Debrunner et al. (1982) and Clem (1999) used Monte Carlo simulations of atmospheric cascades.

cidence direction does not accurately determine the slant depth for all secondary components (Clem et al., 1997). In order to compare results, the commonly used effective vertical cutoff will be employed (Cook et al., 1991).

Stoker (1981) and Lockwood et al. (1974) determined their results from observations using parameterization methods while Clem (1999) and Debrunner et al. (1982) used different Monte Carlo simulations to derive their results. In most cases results agree to within a factor of 2, however the results from Stoker (1981) and Debrunner et al. (1982) are more consistent with each other than any other pair. Lockwood et al. (1974) results deviate considerably from the others in the 1-3 GV region while at higher rigidities the Clem (1999) results are significantly lower. The deviation in the Lockwood et al. (1974) analysis could be due to an unphysical representation of the primary spectrum of protons and alphas used to extract the yield function from observations while it is currently not clear as to the source of the deviation of the Clem (1999) results with respect to the others, although some of the neglected mechanisms described earlier are currently under investigation.

The use of neutron monitor yield functions is not restricted to galactic cosmic rays, but is also very important to the analysis of solar cosmic ray events. High energy nucleons produced in solar mass eruptions propagate through the interplanetary medium and sometimes enter

the Earth's atmosphere. The simultaneous detection of a solar event at different rigidity cutoff locations can provide information relating to the spectra shape, however the value of such information is highly dependent on the yield function accuracy for each location. As discussed in the Monte Carlo section, work in determining an accurate solar neutron yield function continues, however as with the proton yield functions, the results are significantly different. Generally Monte Carlo or theoretical calculations directly determine yield functions and inaccurate results can usually be traced to unphysical models in either the fundamental processes involved in particle transport or in the material composition and geometry. However, inaccurate results from parameterization methods, which extract the yield function through deconvoluting latitude survey data, are usually caused by not knowing the actual primary spectrum or geomagnetic field during the time of the survey. Systematic inaccuracies can also be introduced through unphysical smoothing of latitude survey count rates. Due to the nature of latitude surveys, yield functions derived through the parameterization method are usually less reliable in the lower rigidity regime.

As previously discussed, weighting the yield function (Figure 11) with a chosen primary spectrum produces an associated response function (Figure 12) and the total count rate of a neutron monitor (integral response) is calculated by integrating the response function over rigidity (Figure 13). The response function is a difficult quantity to compare since researchers publish results with different primary spectra depending on the application or observation. The comparison of response functions determined from observations (i.e. parameterization method), assuming the actual yield functions are identical, reflect changes in primary particle spectrum and the geomagnetic field since latitude surveys are rarely performed during the same time and over the same geographical locations. Therefore a quantitative comparison is only possible after a detailed analysis of each response function is performed (Moraal et al., 1989).

As a qualitative comparison Figure 12 displays total response functions at sea-level during solar minimum. As shown, the peak responses vary in the range of 4-7 GV with a median rigidity in the range of 13-17 GV. The Moraal et al. (1989) curve is the result of fitting a Dorman Function to the 1987 survey on the research vessel S.A Agulhas. Numerous surveys were analyzed revealing significant differences indicating a 22 year modulation cycle in the primary spectrum (Moraal et al., 1989, Bieber et al., 1997). The Nagashima et al. (1989) result is also shown for solar minimum. They derived the interstellar galactic spectrum with a power index as a free parameter obtaining the best fit value of 2.59, which is lower than the observed values of 2.75 for protons

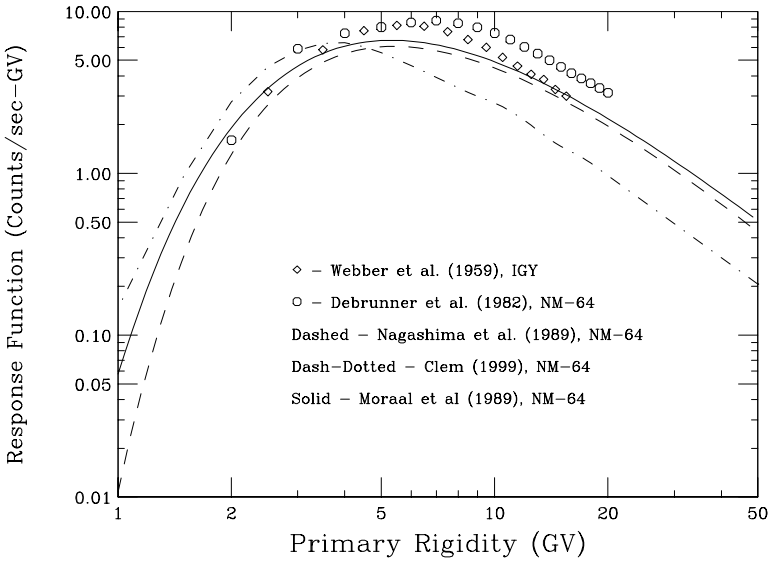

Figure 12. A comparison of different sea-level response functions during solar minimum. The response functions derived by Webber and Quenby (1959), Moraal et al. (1989) and Nagashima et al. (1989) were determined using similar parameterization methods while Debrunner et al. (1982) and Clem (1999) used Monte Carlo simulations of atmospheric cascades. The Webber and Quenby (1959) results were determined with an IGY monitor while the other results displayed were determined with a NM-64 monitor.

and 2.7 for alphas (Swordy, 1993). Nevertheless, the NM-64 results determined from parameterization methods have a very similar shape in particular in the high rigidity regime. The Debrunner et al. (1982) results were determined using the yield function shown in figure 12 folded with the spectrum reported in Raubenheimer et al. (1977). The Clem (1999) results were determined with a galactic spectrum of power index of 2.7 in momentum space for both protons and alphas modulated to solar minimum level. Also shown in Figure 12 is the Webber and Quenby (1959) results which were determined with an IGY monitor and normalized by requiring the count rate to equal 100/sec at 15 GV. As previously discussed the yield function of a IGY monitor is similar, but not identical to a NM-64, which is mainly attributed to a different detection efficiency.

Figure 13 shows data recorded during the 1994-95 Tasmania-Bartol survey using a 3-NM64. The result is typical of prior surveys, showing mainly random deviations at the 0.5% level while others seem rather systematic, such as the deviations in the region of 6-8 GV. Stoker (1995) noted similar humps in airborne surveys, and suggested that obliquely incident particles may be responsible (Rao et al., 1963). Also shown in

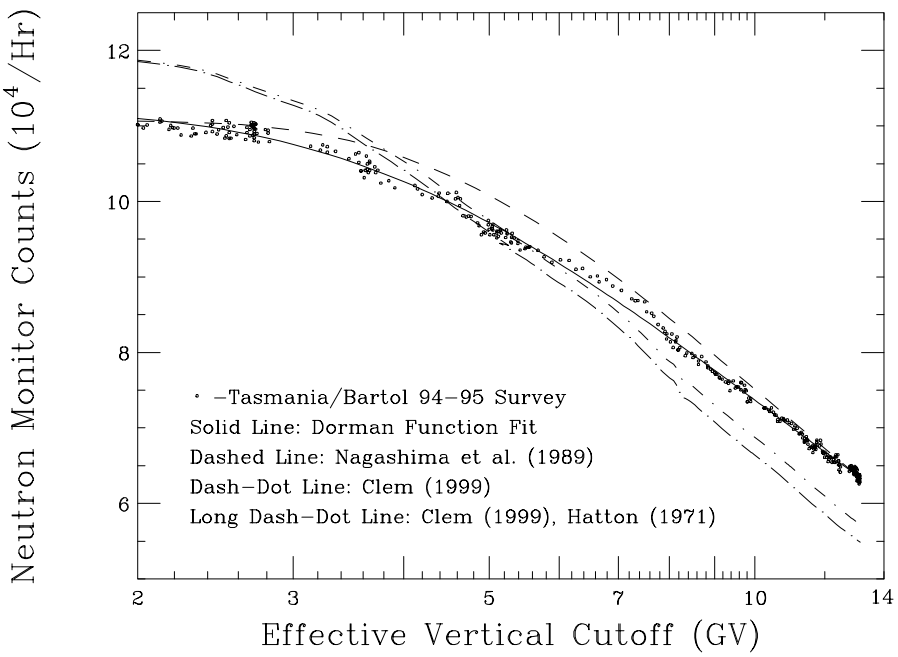

Figure 13. Count rate recorded during the Tasmania-Bartol 1994-95 latitude survey compared with various derived count rates. The solid line was determine using Dorman function fit to the displayed observations. The dashed line represents Nagashima et al. (1989) parameterization for solar minimum epoch. The two dash-dot lines were determined using the Clem (1999) Monte Carlo result with angle dependent cutoffs (Clem et al., 1997) for each location along the survey. The long dash-dot line was determined using the Hatton (1971) neutron monitor detection efficiency with the Clem (1999) atmospheric transport.

Figure 13 are different derived count rates for comparison. The results derived from the Clem (1999 and references therein) Monte Carlo used angle dependent effective cutoffs for different geographical locations along the survey. As shown, the scaled derived count rates have a somewhat steeper slope than observations which could be symptomatic of neglected effects discussed earlier, nevertheless the results produce a similar anomaly within the same rigidity region of observations. The anomaly is the result of a change in the contribution of obliquely incident primary particles to the count rate (Clem et al., 1997, Stoker et al., 1997). For comparison purposes, we display the results using the Hatton (1971) NM64 detection efficiency with the Clem (1999) atmospheric transport Monte Carlo which seems to produce a steeper slope. Also shown is the result of a Dorman function fit to the displayed observations which is represented by the solid line while Nagashima et al. (1989) results are represented by a dashed line. Both of these parameterization techniques ignore the effects of obliquely incident particles

and so the hump anomaly is not reproducible. Even though the overall representation derived by the parameterization techniques is adequate for some purposes, these types of anomalies can significantly affect the derived response function.

7. Summary

Over the past 40 years much progress has been made in providing increasingly accurate neutron monitor yield functions. Even though there are significant disagreements between results of various workers, the understanding of this complex problem is continuously growing. Any physics problem that involves energy ranges of nearly 14 orders of magnitude (near-thermal to 2 TeV) is expected to have many difficulties, however most published results are surprisingly consistent within a factor of 2 while current Monte Carlo calculations differ by roughly 15 percent from latitude survey observations. For the future, achieving a few additional goals could greatly improve our understanding of neutron monitors at the fundamental level and provide clearer insight on how each basic transport mechanism plays a role in defining the inherent features of response functions.

The current work on calibrating a neutron monitor at the Osaka University nuclear accelerator facility is very interesting and is providing exciting results (Koi et al., 1999, Shibata et al., 1997, 1999). More data from measurements at different energies and particle species would be valuable. According to simulations, the neutron monitor detection efficiency of protons and neutrons above 2 GeV are indistinguishable. Therefore, a calibration run at proton accelerator sites with beam energies between 2-200 GeV would be quite useful, in particular when studying the multiplicity distributions. Once the detection efficiency is determined experimentally and a solid theoretical prediction is established for fitting and interpolation purposes, the particle transport of particles through the atmosphere is the only component needed to determine the neutron monitor yield function. Improved communication is needed between independent researchers involved with atmospheric particle transport problems to relay and exchange ideas on their progress and milestones. Arranging informal workshops would allow personal interaction and would hopefully provide fruitful results in establishing a standard transport package.

The continuation of latitude surveys provides important information on the time variation of geomagnetic cutoffs and the primary spectrum, and how these variables affect the derived response function. Re-establishing air borne latitude surveys at different altitudes would

greatly complement the sea-level measurements providing greater constraints on the yield function calculations. The confidence level of yield functions used for mountain neutron monitors would also significantly improve from low altitude (5-10 kft) surveys. It would also be useful to create a data base from all neutron monitor surveys that have been performed so far. The database would be updated each time a new successful survey is completed.

A portable neutron monitor calibrator should be developed to determine the relative responses from station to station. The different local surroundings at each site could attenuate or even augment a neutron monitor count rate, and therefore possibly change the normalization and shape of the yield function. A relative calibration of each station is required at network sites to study spatial and spectral effects in solar events or changes in the primary galactic spectrum (Moraal et al., 2000).

Faster calculations of geomagnetic cutoffs are needed in order to determine angle dependent cutoffs (Lin et al., 1995, Smart et al., 2000). As shown earlier, the angle dependent yield functions show that the contribution of obliquely incident particles is significant (Clem et al., 1997, Stoker et al., 1997), however the computer time required to calculate an angular cutoff grid with adequate resolution is currently about 40 hrs of CPU.

8. Acknowledgements

We want to thank John Bieber, Rolf Bütikofer, Paul Evenson, Hermann Debrunner, Marc Duldig, Alfredo Ferrari, Erwin Flückiger, John Humble, Yasushi Muraki, Roger Pyle, Jim Ryan, Peggy Shea and Pieter Stoker for their suggestions and assistance in this project. We also appreciate the hospitality and support of the International Space Science Institute, Bern. This work was supported by NSF grants OPP-9528122, ATM-9616610, OPP-9724293, and OPP-9805780.

References

Allkofer, O. and P. Grieder: 1984, 'Cosmic Rays on Earth', *Fachinformationszentrum* , Karlsruhe

Badwhar, G.D. and P.M. O'Neill: 1996, 'Galactic Cosmic Radiation Model and Its Applications', *Adv. Space Res.*, **17**, 7-17

Belov, A. V. and A. B. Struminsky: 1997 'Neutron Monitor Sensitivity to Primary Protons below 3 GeV derived from data of Ground Level Events', *Proc. 25th Internat. Cosmic Ray Conf. (Durban)*, 1, 201

Belov, A., A. Struminsky and V. Yanke: 1999, 'Neutron Monitor Response Functions for Galactic and Solar Cosmic Rays', *ISSI Workshop on Cosmic Rays and Earth*, poster presentation and private communication

Bercovitch, M. and B. Robertson: 1966, 'Meteorological factors affecting the counting rate of neutron monitors' *Proc. 9th Internat. Cosmic Ray Conf. (London)*, **1**, 489

Bieber, J. and P. Evenson: 1995, 'Spaceship Earth – An Optimized Network of Neutron Monitors', *Proc. 24th Internat. Cosmic Ray Conf. (Rome)*, **4**, 1316

Bieber, J. and P. Evenson, J. Humble and M. Duldig: 1997, 'Cosmic Ray Spectra Deduced from Neutron Monitor Surveys', *Proc. 25th Internat. Cosmic Ray Conf. (Durban)*, **2**, 45-48

Brown, R.: 1957, 'Neutron Yield Functions of the Nucleonic Component of Cosmic Radiation', *Nuovo Cimento*, 6, 2816

Bütikofer, R. and E. Flückiger: 1999, 'Pressure Correction of GLE Measurements in Turbulent Winds', *Proc. 26th Internat. Cosmic Ray Conf. (Salt Lake City)*, **6**, 395

Carmichael, H., M. Shea and R. Peterson: 1969a, 'III. Cosmic-ray survey in Western USA and Hawaii in summer, 1966', *Canadian Journal of Physics*, **47**, 2057

Carmichael, H. and M. Bercovitch: 1969b, 'V. Analysis of IQSY cosmic-ray survey measurements', *Canadian Journal of Physics*, **47**, 2073

Clem, J.M., J.W. Bieber, P. Evenson, D. Hall, J.E. Humble, M. Duldig: 1997, 'Contribution of Obliquely Incident particles to Neutron Monitor Counting Rate', *Journal of Geophysical Research*, **102**, 26919

Clem, J.M.: 1999, 'Atmospheric Yield Functions and the Response to Secondary Particles of Neutron Monitors' *Proc. 26th Internat. Cosmic Ray Conf. (Salt Lake City)*, **7**, 317

Cook, D.J., J.E. Humble, M.A. Shea, D.F. Smart, N. Lund, I.L. Rasmussen, B. Byrnak, P. Goret and N. Petrou: 1991, 'On Cosmic Ray Cut-Off Terminology', *Nuovo Cimento* **14C**, 213-234

Debrunner, H. and E. Brunberg: 1968, 'Monte Carlo Calculation of Nucleonic Cascade in the Atmosphere', *Canadian Journal of Physics*, **46**, 1069

Debrunner, H., J. Lockwood and E. Flückiger: 1982, *8th Europe Cosmic Ray Symp.*, Rome, unpublished

Debrunner, H., J.A. Lockwood, C. Barat, R. Bütikoker, J.P. Dezalay, E. Flückiger, A. Kuznetsov, J.M. Ryan, R. Sunyaev, O.V. Terekhov, G. Trottet and N. Vilmer: 1997, 'Energetic Neutrons, Protons, and Gamma Rays During the 1990 May 24 Solar Cosmic-Ray Event', *Astrophysical Journal*, **479**, 997

Debrunner, H.: 2000, 'Solar Neutron Measurements with Neutron Monitors', *Space Sci. Rev*, (this volume)

Dorman, L.: 1957, 'Cosmic Ray Variations', *State Publishing House for Technical and Theoretical Literature*, **102**

Dorman, L.I.: 1970, 'Coupling and barometer coefficients for measurements of cosmic ray variations at altitudes of 260-400 mb', *Acta Phys. Acad. Sci. Hung.*, **29 (suppl 2)**, 233

Dorman, L. and V. Yanke: 1981, 'The Coupling Functions of NM-64 Neutron Supermonitor', *Proc. 17th Internat. Cosmic Ray Conf. (Paris)*, **4**, 326

Duldig, M.: 2000, 'Muon Observations', *Space Sci. Rev*, (this volume)

Engel, J., T.Gaisser, P. Lipari and T.Stanev: 1992, *Phys. Rev.*, 'Nucleus-Nucleus Collisions and Interpretation of Cosmic Ray Cascades', **D46**, 5013

Fassò, A., A. Ferrari, A. Ranft, P.R. Sala, G.R. Stevenson and J.M.Zazula: 1993, 'A comparison of FLUKA simulations with measurements of fluence and dose in calorimeter structures', *Nuclear Instruments and Methods*, **A 332**, 459

Fassò, A., A. Ferrari, A. Ranft and P.R. Sala: 1997, *Proceeding of the 2nd workshop on Simulating Accelerator Radiation Environment*, SARE-2, CERN-Geneva, October 9–11 1995, CERN Divisional report **CERN/TIS-RP/97-05**, 158

Fisk, L.A. and W.I. Axford: 1969, 'Solar Modulation of galactic cosmic rays I.', *J. Geophys. Res. Space Physics*, **74**, 4973

Flückiger, E.: 1977, 'Theoretical Spectra of Cosmic Ray Neutrons in the Atmosphere for the Energy Range 50 MeV $\leq$ E $\leq$ 100GeV', *Proceedings of the 15th International Cosmic Ray Conference (Plovdiv)*, **4**, 144

Fonger, W.:1953, 'Cosmic Radiation Intensity-Time Variations and Their Origin. II. Energy Dependence of 27-Day Variation', *Physical Review*, **91**, 351

Gaisser, T.: 1990, 'Cosmic Rays and Particle Physics', *Cambridge University Press*

Garcia-Munoz, M., P. Meyer, K. R. Pyle, J. A. Simpson, and P. Evenson: 1986, 'The Dependence of Solar Modulation on the Sign of the Cosmic Ray Particle Charge', *Journal of Geophysical Research* ,**91**, 2858,

Hatton, C.J.: 1971, 'The Neutron Monitor', *Progress in Elementary Particle and Cosmic Ray Physics*, **X**, American Elsevier Publishing Company

Iucci, N., G. Villoresi, L. Dorman and M. Parisi: 1999, 'Cosmic Ray Survey to Antarctica and Coupling Functions for Neutron Component Near Solar Minimum (1996-1997) 2. Meteorological Effects and Correction of Survey Data', *Proceedings of the 26th International Cosmic Ray Conference (Salt Lake City)*, 7, 321

Koi, T., Y. Muraki, K. Masuda, Y. Matsubara, S. Sakakibara, T. Sako , T. Murata, H. Tsuchiya, Y. Kato, A. Yuki, S. Shibata, Y. Munakata , H. Sakai, T. Nonaka, T. Ohnishi, K. Hatanaka, and T. Wakasa: 1999, 'Attenuation of Solar Neutrons in the Air Determined by an Accelerator Experiment', *Proceedings of the 26th International Cosmic Ray Conference (Salt Lake City)*, **7**, 325

Lockwood, J., W. Webber and L. Hsieh: 1974, 'Solar Flare Proton Rigidity Spectra Deduced from Cosmic Ray Neutron Monitor Observations', *Journal of Geophysical Research*, **79**, 4149

Lin, Z., J.W. Bieber and P. Evenson: 1995, 'Electron trajectories in a model magnetosphere: Simulation and observation under active conditions', *Journal of Geophysical Research*,**100**, 23543

Moraal, H., M.S. Potgieter, P.H. Stoker and A.J.van der Walt: 1989, 'Neutron Monitor Latitude Survey of Cosmic Ray Intensity During the 1986/1987 Solar Minimum,' *Journal of Geophysical Research*, **94**, 1459

Moraal, H., A. Belov and J.M. Clem: 2000, 'Design and coordination of multi-station international neutron monitor networks', *Space Sci. Rev*, (this volume)

Nagashima, K., S. Sakakibara and K. Murakami: 1989, 'Response and Yield Functions of neutron Monitor, Galactic Cosmic Ray Spectrum and Its Solar Modulation, Derived from all the Available World-Wide Surveys', *IL Nuovo Cimento*, **12C**, 173

Pyle, R, P. Evenson, J.W. Bieber, J.M. Clem, J.E. Humble, and M.L. Duldig: 1999, 'The Use of ^{3}He Tubes in a Neutron Monitor Latitude Survey', *Proceedings of the 26th International Cosmic Ray Conference (Salt Lake City)*, **7**, 386

Rao, U.R., K.G. McCraken and D. Venkatesan: 1963, 'Asymptotic Cones of Acceptance and Their Use in the Study of the Daily Variation of Cosmic Radiation', *Journal of Geophysical Research*, **68**, 345

Raubenheimer, B. and P. Stoker: 1974, 'Various aspects of the attenuation coeficient of a neutron monitor', *Journal of Geophysical Research*, **79**, 5069

Raubenheimer, B. and E. Flückiger: 1977, 'Response Functions of a Modified NM-64 Neutron Monitor', *Proceedings of the 15th International Cosmic Ray Conference (Plovdiv)*, **4**, 151

Raubenheimer, B., E. Flückiger, C. Mischke and M. Potgieter: 1980, 'Comparison between the experimental and theoretical responses of neutron monitors', *South Africa Journal of Physics*, **3**, 29

Raubenheimer, B, F. Van Niekerk and M. Potgieter: 1981, 'The Calculation of Differential Response Functions from Latitude Surveys. I: Theory', *Proc. 17th Internat. Cosmic Ray Conf. (Paris)*, **4**, 321

Rossi, B.: 1948, 'Interpretation of Cosmic Phenomena', *Reviews of Modern Physics*, **20**, No 3

Sandström, A.E.,: 1958, 'Cosmic Ray Soft Component Measurements During a Flight from Scandinavia Across the North Pole and Around Asia and Europe', *Supplmento Al Nuovo Cimento* , **VIII**, 363

Seo, E., J.F. Ormes, R.E. Streitmatter, S.J. Stochij, W.V. Jones, S.A. Stephens and T. Bowen: 1991, 'Measurement of Galactic Cosmic Ray Proton and Helium Spectra During the 1987 Solar Minimum', *Astrophysical Journal*, **378**, 763

Shen, M.:, 1968, 'Neutron production in Lead and Energy Response of Neutron Monitor', *Supplmento Al Nuovo Cimento* , **VI**, 1177

Simpson, J.: 1948, 'The Latitude Dependence of Neutron Densities in the Atmosphere as a Function of Altitude', *Phys. Rev.*, **73**, 1389

Shibata, S.: 1994, 'Propagation of solar neutrons through the atmosphere of the Earth', *Journal of Geophysical Research*, **99**, 6651

Shibata, S., Y. Munakata, R. Tatsuoka, Y. Muraki, Y. Matsubara, Sakakibara, T. Koi, T. Sako, A. Okada, T. Murata, I. Imaida, H.Tsuchiya, Y. Ishida, H. Sakai, T. Wakasa, T. Nonaka, T. Ohnishi, and K. Hatanaka: 1997 'Calibration of Neutron Monitor using an Accelerator', *Proc. 25th Internat. Cosmic Ray Conf. (Durban)*, **1**, 45

Shibata, S., Y. Munakata, R. Tatsuoka, Y. Muraki, Y. Matsubara , K. Masuda, T Koi, T. Sako, A. Okada, T. Murata, H. Tsuchiya , I. Imaida, T. Hoshida, Y. Kato, A. Yuki, S. Ohno, K. Hatanaka , T. Wakasa, H. Sakai, T. Nonaka, T. Ohnishi and Y. Ishida: 1999, 'Calibration of Neutron Monitor using Accelerator Neutron Beam', *Proceedings of the 26th International Cosmic Ray Conference (Salt Lake City)*, **7**, 313

Smart, D.: 2000, 'Cutoff Rigidites in the Geomagnetic Field', *Space Sci. Rev*, (this volume)

Stoker, P.H.: 1981, 'Primary Spectral Variations of Cosmic Rays above 1 GeV' *Proc. 17th Internat. Cosmic Ray Conf. (Paris)*, **4**, 193

Stoker, P.H.: 1995, 'Neutron Monitor Latitude Surveys, Response Functions and 22-Year Modulation', *Proceedings of the 24th International Cosmic Ray Conference (Rome)*, **4**, 1082

Stoker, P., J. Clem, J.W. Bieber and P. Evenson: 1997, 'Apparent Geomagnetic Cutoffs and the Cosmic Ray Anomaly in the Cape Town Region', *Proc. 25th Internat. Cosmic Ray Conf. (Durban)*, **2**, 385

Stoker, P., L. Dorman, J. Clem: 2000, 'Neutron Monitor Design Improvements', *Cosmic Rays and Earth*, ISSI, chapter ???

Sullivan, J.D.: 1971, 'Geometrical Factor and Directional Response of Single and Multi-element Particle Telescopes', *Nuclear Instruments and Methods*, **95**, 5

Swordy, S.: 1993, 'Cosmic Ray Observations Below 10^{14} eV', *Proceedings of the 24th International Cosmic Ray Conference (Calgary)*, OG Rapporteur paper, **5**, 243

Villoresi, G., N. Iucci, M.I. Tyasto, L.I. Dorman, F. Re, F. Signoretti, N. Zangrilla, S. Cecchini, M. Parisi, C. Signorini, O.A. Danilova, and N.G. Ptitsyna: 1997, 'Latitude Survey of Cosmic Ray Nucleonic Component (Italy-Antarctic, 1996-1997)' *Proc. 25th Internat. Cosmic Ray Conf. (Durban)*, **2**, 421

Webber, W.R. and J.J. Quenby: 1959, 'On the Deviation of Cosmic Ray Specific Yield Functions',*Phil Mag*, **4** 654

Yanke V.G.: 1980, 'On the Theory of Geophysical Effects of secondary Cosmic Radiation', Cand. Thesis, IZMIRAN, Moscow, 1980 (in Russian).

Zombeck, M.: 1982, 'Handbook of Space Astronomy and Astrophysics', *Cambridge University Press*